Technical Report

R 813

Sponsored by

DIRECTOR OF NAVY LABORATORIES

June 1974

CIVIL ENGINEERING LABORATORY
NAVAL CONSTRUCTION BATTALION CENTER
Port Hueneme, CA 93043

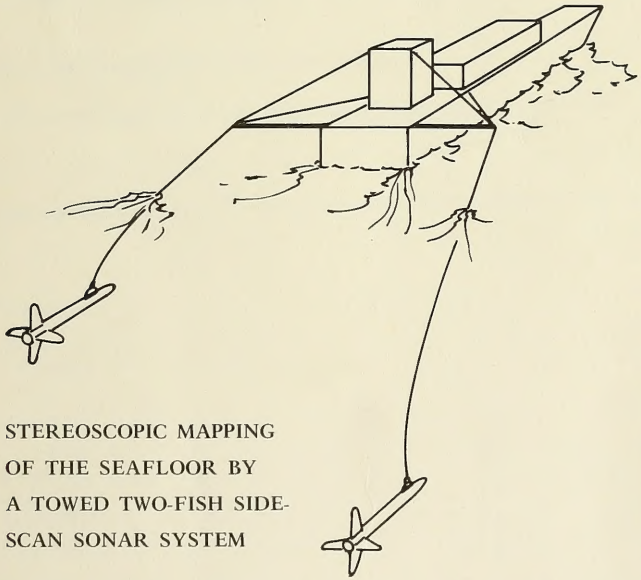

STEREOSCOPIC MAPPING OF THE SEAFLOOR BY A TOWED TWO-FISH SIDE-SCAN SONAR SYSTEM

by R. D. Hitchcock

Unclassified

SECURITY CLASSIFICATION OF THIS PAGE (When Data Entered)

REPORT DOCUMENTATION PAGE		READ INSTRUCTIONS BEFORE COMPLETING FORM
1. REPORT NUMBER TR-813	2. GOVT ACCESSION NO.	3. RECIPIENT'S CATALOG NUMBER
4. TITLE (and Subtitle) STEREOSCOPIC MAPPING OF THE SEAFLOOR BY A TOWED TWO-FISH SIDE-SCAN SONAR SYSTEM		5. TYPE OF REPORT & PERIOD COVERED June 1973—June 1973 (2 weeks) 6. PERFORMING ORG. REPORT NUMBER
7. AUTHOR(s) R. D. Hitchcock		8. CONTRACT OR GRANT NUMBER(s)
9. PERFORMING ORGANIZATION NAME AND ADDRESS CIVIL ENGINEERING LABORATORY Naval Construction Battalion Center Port Hueneme, California 93043		10. PROGRAM ELEMENT, PROJECT, TASK AREA & WORK UNIT NUMBERS ZF61-512-001-025
11. CONTROLLING OFFICE NAME AND ADDRESS Director of Navy Laboratories Washington, D. C. 20376		12. REPORT DATE June 1974 13. NUMBER OF PAGES 27
14. MONITORING AGENCY NAME & ADDRESS(if different from Controlling Office)		15. SECURITY CLASS. (of this report) Unclassified 15a. DECLASSIFICATION/DOWNGRADING SCHEDULE

16. DISTRIBUTION STATEMENT (of this Report)

Approved for public release; distribution unlimited.

17. DISTRIBUTION STATEMENT (of the abstract entered in Block 20, if different from Report)

18. SUPPLEMENTARY NOTES

19. KEY WORDS (Continue on reverse side if necessary and identify by block number)

Seafloor mapping, sonar mapping, seafloor map, contour map, stereo-sonar plot, digital computer plot, side-scan sonar, towed fish.

20. ABSTRACT (Continue on reverse side if necessary and identify by block number)

Sea trials were conducted to test the concept of constructing a seafloor contour map by interfacing a manual stereo-sonar plotter with a digital computer. The at-sea work utilized a pair of 100-kHz, side-scan, sonar fish towed at a lateral separation of 42 feet. Real-time data on near-bottom scanning contained mutual interference effects which prevented the stereoscopic fusing of corresponding sonar images. System component

continued

DD FORM 1 JAN 73 1473 EDITION OF 1 NOV 65 IS OBSOLETE

Unclassified

SECURITY CLASSIFICATION OF THIS PAGE (When Data Entered)

20. Continued

errors were obtainable with repeated scannings of an artificial target array. Random errors in the horizontal component of the fish-pair vector, $\vec{B}$, were computed to be around 2.6 feet. Random errors in the vertical component of $\vec{B}$ were around 7.5 feet. These errors were associated with an average off-bottom distance of 70 feet and a fish-pair lateral separation of 43 feet. Because of the marked sensitivity of target-elevation error to the horizontal and vertical errors in $\vec{B}$, the stereo plotting of seafloor contours could not yield useful results. It is concluded that measurement of the components of $\vec{B}$ must yield errors less than 0.5 foot in 40 feet. It is further concluded that fish heave must be within 4 feet peak-to-peak and that mutual interference effects must be absent if stereo plotting of sonar-image pairs is to be performed successfully.

CONTENTS

INTRODUCTION

The concept of constructing a seafloor contour map by means of stereo-sonar imagery has been investigated by Mittleman and Malloy of the Civil Engineering Laboratory, Naval Construction Battalion Center, Port Hueneme, California,[a] [1]. This investigation was mainly theoretical but included some qualitative results of scanning the seafloor with a pair of laterally separated, side-looking, sonar fish. Because of virtually no precision in the estimate of fish separation, it was not possible to compute relative target elevations. However, direct stereoscopic viewing of some of the sonar-image pairs did result in the blending of seafloor features into a three-dimensional illusion. From these results it was concluded that stereo-sonar techniques could be used for contour mapping of the seafloor in the same way that stereo-photo techniques are used to map land areas.

In June 1973, further sea trials were conducted by CEL in an attempt to study quantitatively the concept of stereo-sonar mapping. Two basic improvements in stereo-sonar technology were made for these sea trials: (1) a side-scan system was used having a sonar frequency lower by an order of magnitude than the frequency of the system used in the investigation of Reference 1; and (2) the lateral separation of the two sonar fish was doubled. Lowering the sonar frequency allowed coverage of a relatively large seafloor area, yielding, in turn, more data for a given operational period. It was assumed that increasing the lateral separation of the two sonar fish and towing at relatively short cable lengths would maintain a constant horizontal separation of the two fish; and, hence, target elevation errors would be less than 3 feet in 100 feet.

The June 1973 work described in this report was performed to produce sonar-image pairs which, not only would blend into a three-dimensional picture when viewed stereoscopically, but also would allow digital computation of seafloor contour data by interfacing the computer with the settings made by the stereo operator.

THE STEREO-SONAR PROBLEM

Stereo plotting to construct land contour maps from stereo-photo pairs is used because a human observer with his two eyes can pick out points of equal elevation with high precision. He can do this more efficiently than a machine and at lower cost. A machine subsystem can then be used to take the stereo observer's adjustments and produce numerical values for the contours.

A basic problem in side-looking stereo-sonar mapping is the requirement that the seafloor be scanned a line at a time, instead of an area at a time as in aerial stereo-photo mapping of land topography. This requirement imposes a severe restriction on the allowable magnitude of system errors because in the line-scanning system, information is obtained at a much slower rate than in the area-scanning system.

Another problem in stereo-sonar is that sonar measures range instead of angle as in optical imaging. Whereas the eye-brain system directly yields precise information on elevation differences if the image pair is obtained optically, in the stereo viewing of sonar image pairs, the eye-brain system yields false elevation differences. Hence, it becomes necessary to transform the false elevations to true elevations by using a set of equations. As outlined in Reference 2, this has been done for radar-stereo imagery. Side-looking airborne radar measures range in the same way that side-scan sonar does; that is, by measuring the travel time of the signal.

Further problems arise when an attempt is made to view stereo-sonar imagery in a stereoscope and to create a three-dimensional illusion. The result is

[a] Designation prior to January 1, 1974: Naval Civil Engineering Laboratory, Port Hueneme, California.

usually not a three-dimensional picture. This is due, in the case of large targets, high resolution, and near-bottom scanning, to different rates of parallax change[b] between shadow and target signals [3]. In the case of high-flying stereo-sonar scanning, where the essential imagery is contained in target returns, the three-dimensional illusion is created only if suitable contrast and resolution are present [1].

Figure 1 shows the geometry of the stereo-sonar system. The equations which take the echo ranges, R_1 and R_2, to the relative target elevation are the following:

$$B = (h^2 + H^2)^{1/2} \quad (1)$$

$$\theta = \tan^{-1}(h/H) \quad (2)$$

$$\xi = \left\{(R_2^2 - R_1^2)/2B\right\} - (B/2) \quad (3)$$

$$\eta = (R_1^2 - \xi^2)^{1/2} \quad (4)$$

$$y_t = -(\xi + B)\sin\theta + \eta\cos\theta \quad (5)$$

$$x_t = (\xi + B)\cos\theta + \eta\sin\theta \quad (6)$$

where $B = |\vec{B}|$

$\vec{B}$ = fish-pair vector

θ = direction of $\vec{B}$, relative to horizontal (positive for fish no. 1 above fish no. 2)

h = vertical component of $\vec{B}$

H = horizontal component of $\vec{B}$

y_t = vertical distance of target below fish no. 2 (positive for targets below fish no. 2)

The sixth equation yields, x_t, the horizontal distance of the target from fish no. 2. However, unless a shore-based fish navigation system is used, this computation is not important. Presumably, it is much easier to keep systematic fish-depth errors below a yard or so than it is to keep the systematic horizontal errors (relative to shore or a fixed seafloor point) below several yards.

Figure 2 is a schematic diagram of a contour plotting system utilizing the principles of the double-projection, direct-viewing stereoplotter. In the stereo plotting of seafloor contours using side-scan data, the operator would begin somewhere on the crosstrack line passing through the first along-track point of the sonar-stereo scan. Labeling each recognizable target point on this first crosstrack line, the operator would move the viewing screen vertically and horizontally until the no. 1 target point appeared to lie in the plane of and at the center of the screen. His eye-brain system, with the aid of conventional stereo goggles (for example, red-green), would make this possible. Mechanical linkages between viewing screen and the computer would cause the sonar ranges, R_1 and R_2, to be fed into the computer in feet. (Of course, with optical stereo images in front of the two projectors, no computer is necessary; and the operator simply makes a mark on the map surface directly below the center of the viewing screen.) With stereo-sonar images in front of the projectors, the computer would take R_1 and R_2 and, using Equations 1 through 6, calculate the target position.

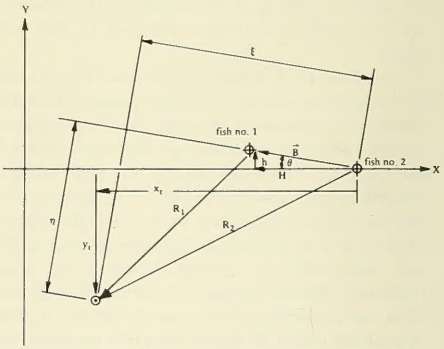

Figure 1. Geometry of stereo-sonar system for computation of target position.

The problem with the procedure described above is that the operator would have to go through all of the target points on each crosstrack line, and then instruct the computer to arrange the

[b] Rate = $\frac{\text{Change in parallax (feet)}}{\text{Change in range (feet)}}$

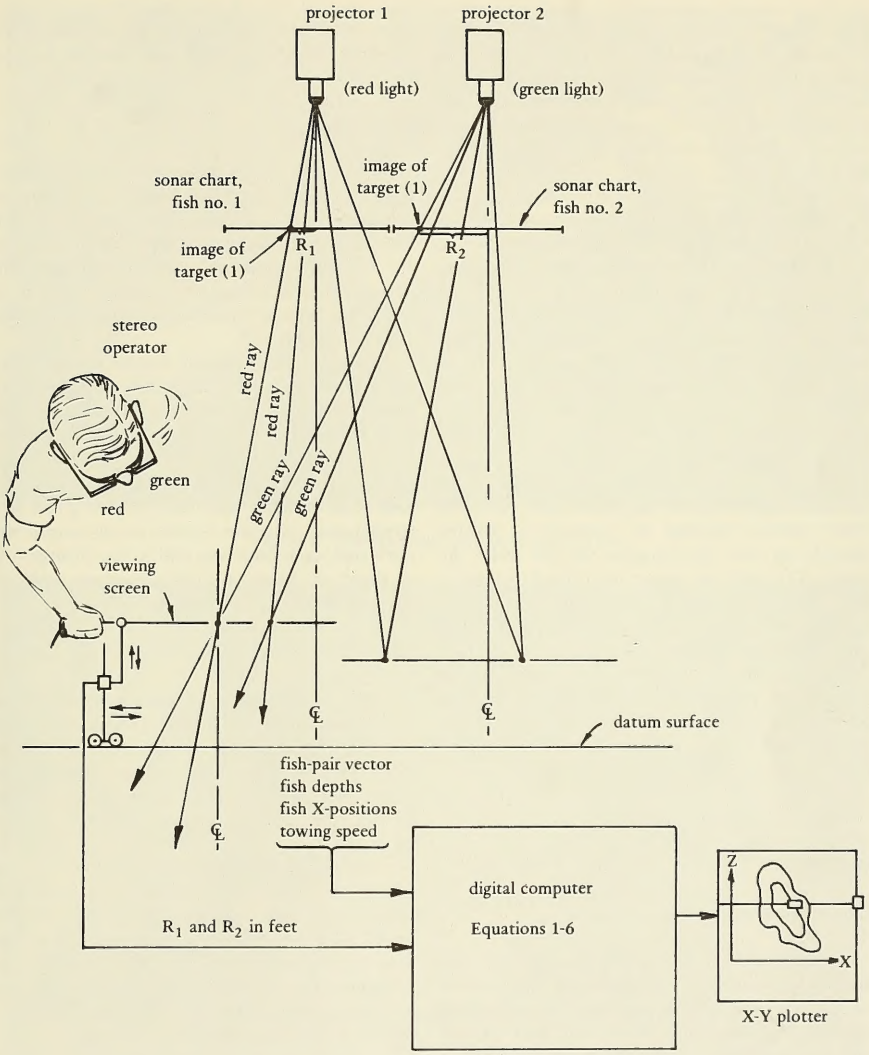

Figure 2. Schematic of double-projector direct-viewing stereo plotter.

target-position data into equal-elevation sets. Feeding these sets, successively, to an X-Y plotter would then yield the usual type of contour map. With optical stereo pairs in front of the projectors, this final sorting process is unnecessary because the operator directly plots equal-elevation points as he constructs the map.

The brute-force procedure is to directly measure R_1 and R_2 without using a stereo-projector/computer system (such as in Figure 2); but the assumption is, and has been from the beginning of this investigation, that the stereo-viewing approach will be faster and less expensive. This assumption is based on the reason used in stereo-photo plotting: it is easier to match corresponding target points by stereoscopic viewing than by (1) looking at the separate images, (2) picking out what appear to be matching points, and (3) making measurements directly on the image surface with a calibrated scale.

Hence, provided system errors are under a specified magnitude, the practical value of stereo-sonar contour mapping by stereoscopic viewing depends on how photographic we can make the images. The sonar-pair images must blend together in such a way that there is an insignificant probability of matching images which do not correspond. The image-definition problem is as important as the fish-vector measurement problem. Even with infinite precision in the measurement of $\vec{B}$ and the fish positions in a shore-based reference frame, if the imagery cannot be fused into a three-dimensional illusion, stereo plotting is not workable.

SEA TRIALS

Sonar Equipment

The towed sonar system consisted of two side-looking sonar fish operated through a dual-channel transceiver/recorder having a wet-paper chart readout. Each sonar fish was a Klein Model 402A, shown in Figure 3 on board the towing vessel. The deck equipment was a Klein Model 401 recorder (Figure 4) and a specially built auxiliary unit for operating both fish simultaneously.

Each sonar fish was operated at 100 kHz and up to a maximum of 10 pps with pulse length of 0.1 msec. The two-fish system, including two 300-foot electromechanical cables, was furnished under a lease agreement with Klein Associates, Inc., Salem, New Hampshire.

Tow System

A schematic of the tow system is shown in Figure 5. A 42-foot, 2-inch-diameter steel pipe was attached to the stern of an LCM-8 and stabilized by lines connecting the ends of the pipe to the gunnels and the wheel house. The starboard section of this outrigger system is shown in Figure 6, with the fish under tow. Towing speed was held at approximately 2 knots.

The required tow-cable lengths were estimated for the desired depths and trailing distances of the two fish. The estimates were based on assumed values of hydrodynamic parameters, such as drag and cable buoyancy. The Klein electromechanical cable, having an outside diameter of 3/8 inch and utilizing a fiber glass strain member, was used for towing and signal transmission. After the required towing lengths were calculated, each cable was tied to the outrigger pipe as shown in Figure 6; and the excess cable was wrapped around a gunnel bitt and coiled on deck.

Stereo-Sonar Operations

All of the stereo-sonar data were obtained at two near-shore areas. One area in the vicinity of CEL was about 2.5 nautical miles offshore with a depth of about 100 feet. The other area, just outside the surf zone at the Carpinteria beach about 22 nautical miles up the coast from CEL, had an average depth of about 25 feet.

Because the 100-foot-depth seafloor area near CEL is essentially featureless, an array of artificial sonar targets was implanted. Four reflectors were spaced about 500 feet apart, connected by a bottom-lying 1-inch-diameter wire rope. Each reflector was a 2,600-pound concrete block to which was attached a buoyant 35-inch-diameter aluminum sphere. A schematic of the array is shown in Figure 7.

The 100-foot-depth area was chosen to permit same-side stereo scanning with maximum bottom coverage. The tow-cable lengths were adjusted to produce the geometry shown approximately in Figure 8. Tow-cable lengths for fish no. 1 and no. 2 were adjusted to 80 and 20 feet, respectively, yielding depths of roughly 30 and 20 feet, respectively.

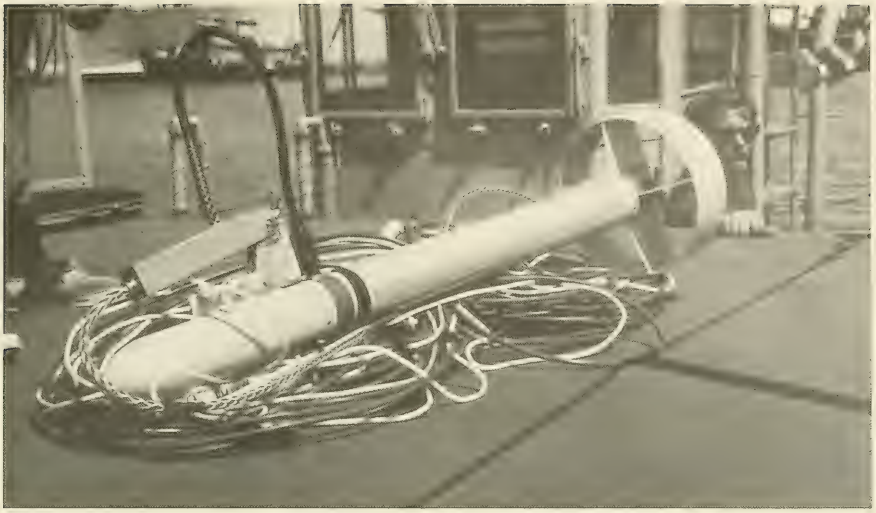

Figure 3. Side-scan fish with tow/signal cable.

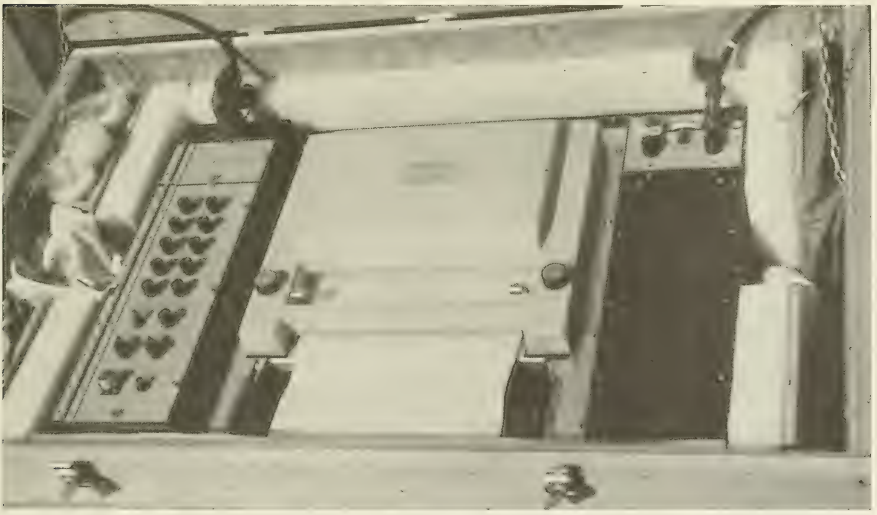

Figure 4. Sonar transceiver/recorder.

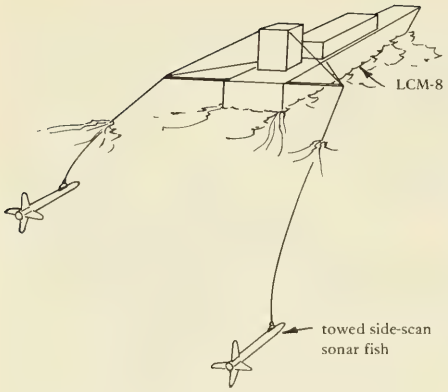

Figure 5. Stereo-sonar tow system schematic.

Although the manufacturer's specifications state that the vertical sonar angle, θ_s, is 20 degrees, it was assumed that in the 100 to 200-foot range adequate returns would be generated within a vertical angle of about 50 degrees.

To maximize stereo target-detection probability, the fish-vector $\vec{B}$ was oriented toward the assumed target area (marked by surface floats as shown in Figure 7). This situation, of having $\vec{B}$ slanted down instead of up (see Figure 8), creates a bad situation with respect to the precision of determining target elevation, y_t. If the target is on the line passing through the two fish (that is, on the extension of $\vec{B}$), the theoretical random error in y_t becomes infinite. This is intuitively clear and is shown quantitatively by the error-propagation equations of Appendix A. It was believed, however, that the risk of having large errors in y_t was worth taking because of the small stereo target-detection probability associated with a slanted-up fish vector.

It was also suspected that a relatively large value of the elevation angle, β_i (see Figure 8) would decrease the one-fish target-detection probability because of the small shadow associated with a large β_i. A low-β (low-flying) situation would cause large errors in y_t.

Hence, with all of the above considerations, the geometry of Figure 8 appeared to be optimum. A better geometry might have been opposite-side stereo (assuming that image blending is possible) with a horizontal $\vec{B}$ component of around 200 feet. A

Figure 6. Starboard section of towing outrigger.

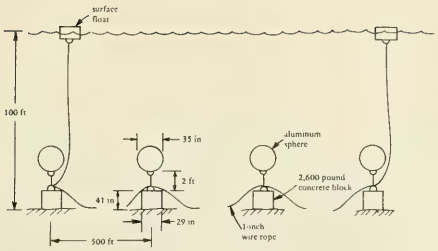

Figure 7. Schematic of artificial target array.

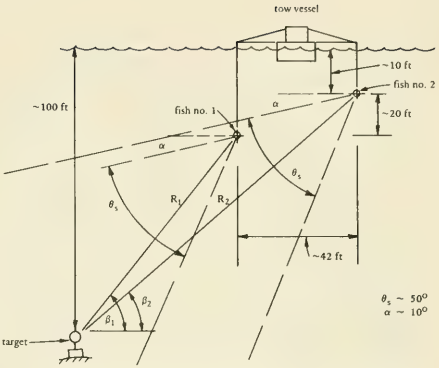

Figure 8. Geometry of same-side stereo scanning at 100-foot-depth site.

horizontal component of this extent was, however, not feasible. Analysis of outrigger statics and dynamics showed that a 42-foot length was the maximum tolerable.[c]

The other near-shore area, just beyond the surf, was chosen because of the abundance of prominent rock outcroppings. Although low-flying stereo scanning was required, with its attendant problems of grounding probability and error propagation, it was believed that the highly contrasted imagery would demonstrate the feasibility of fusing sonar charts into a three-dimensional illusion.

RESULTS OF SEA TRIALS

The sea trials covered a period of 6 days, during which 15 hours were actually devoted to stereo scanning. Out of these 15 hours, about 3 hours yielded data which appeared to be usable in Equations 1 through 5. The data were those image points on the sonar charts which were recognizable as either the artificial targets, including the bottom-lying wire rope, or a rock outcropping.

The remaining 10 hours of sonar scanning yielded imagery which did not contain clearly identifiable targets. Most of this data resulted from the existence of sea state 1 or greater during that time. From the sonar-chart readout and direct observation of outrigger and tow-cable motion during sea state 1 or greater, it was estimated that vertical motion of either one of the sonar fish was in excess of 4 feet, peak-to-peak. At the 100-foot-depth site, with approximate sea state 0, peak-to-peak vertical motion of an individual fish appeared to be under 4 feet, and imagery was produced in the sonar readout which could be blended into a three-dimensional illusion.[d] Figure 9 shows a section of stereo-sonar imagery of the 100-foot-depth target array for sea state 0.

Table 1 gives the results of 10 side-looking stereo sweeps at the 100-foot-depth site. The maximum possible number of measurements on a given sonar reflector is five. Crosstalk and mutual interference effects were minimized by using different tow-cable lengths and, thus, staggering the two fish out of each other's beam.

[c] A sea test was conducted to see if a pair of manned small boats could be towed at a constant separation of 50 feet. With a tension line between the two boats, their separation could be held constant in a harbor tow; but, in the open sea, even small-wave action made it impossible to maintain a constant lateral separation.

[d] Long sections of the 1-inch wire rope are clearly discernible in the sonar charts. Because of the high resolution and contrast of the wire-rope imagery, three-dimensional blending is possible. However, the resolution of the sphere-block targets was not sufficient to yield three-dimensional imagery.

Table 1. Results of Stereo-Sonar Scans of 100-Foot-Depth Target Array

(Assumed value of horizontal stereo baseline, **H**, is 42.00 feet.)

Time	Target[a]	Fish No. 1 Echo Range, R_1 (ft)	Fish No. 2 Echo Range, R_2 (ft)	Fish Pair Depth Difference, h (ft)[b]	Computed Target Elevation, y_t (ft)	Spread In Target Elevations, y_t (ft)
0807	SB1	117.59	116.10	−19.17	105.88	9.80
0807	WR1	120.70	165.77	−19.16	95.53	9.77
0833	SB1	118.11	162.14	−21.75	115.68	
0833	WR1	121.73	165.77	−19.16	105.30	
0734	SB2	94.28	140.38	−19.69	70.77	12.09
0734	WR2	97.91	144.01	−19.69	72.67	24.92
0831	SB2	107.23	154.37	−19.68	65.19	
0831	WR2	112.93	158.51	−20.20	92.72	
0838	SB2	138.31	186.49	−18.13	72.95	
0838	WR2	142.97	189.60	−16.58	69.07	
0853	SB2	55.43	95.83	−23.83	77.28	
0853	WR2	62.16	101.01	−23.83	84.56	
0719	WR2	102.05	147.64	−18.13	67.80	
0829	SB3	110.86	158.00	−19.68	66.73	57.37
0829	WR3	113.96	160.59	−19.69	68.05	15.60
0648	SB3	146.60	194.26	−17.61	74.31	
0732	WR3	138.31	187.52	−21.24	83.65	
0720	SB3	88.06	126.91	−18.65	97.46	
0749	WR3	155.41	202.55	−18.65	81.71	
0839	SB3	143.49	191.67	−17.61	73.10	
0851	SB3	101.01	145.56	−29.01	124.10	
0750	SB4	117.07	163.69	−18.13	64.53	25.70
0750	WR4	123.81	170.95	−17.61	65.49	30.20
0827	SB4	125.36	171.98	−20.21	74.54	
0827	WR4	130.02	176.13	−19.69	89.45	
0842	SB4	121.22	165.77	−17.61	90.23	
0849	WR4	105.68	150.74	−20.73	95.69	
0849	SB4	99.98	145.56	−20.72	88.01	

[a] SB = sphere-block; WR = wire rope on bottom next to SB.
[b] Average value: h = −19.85.

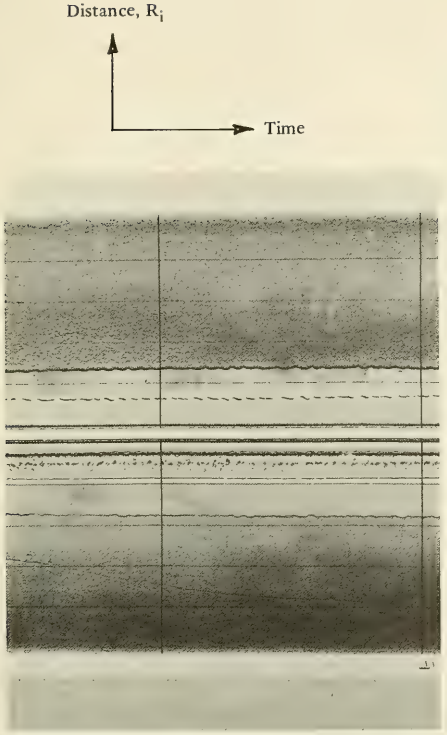

Distance between horizontal lines = 15 meters
Time between vertical lines = 2 minutes

Figure 9. Two-fish sonar-chart readout of artificial target array.

In the next-to-last column of Table 1, the computed relative elevation, y_t, is given for every time the image appears. The parameter, **h**, of Equation 1 was calculated by taking the difference between the off-bottom heights of the two fish. This calculation, of course, assumes a flat bottom. The horizontal component of $\vec{B}$ was assumed to be the outrigger length, 42 feet.

Table 1 reveals a marked scatter in the set of y_t values for any given target. For example, the target, SB3, has five computed values of y_t, and the difference between minimum and maximum y_t is 57.37 feet. The difference value, Δy_t, is given in the last column of Table 1 for each target. The smallest Δy_t is 9.77 feet.

Presumably, the large spread in y_t for a given target is the result of (1) errors in the measurement of the components of $\vec{B}$, and (2) target points lying on or near the line through the two fish. Systematic errors in **h** could be expected since this parameter had to be computed from off-bottom fish heights. Having target points on or near the extension of $\vec{B}$ was evidently the result of "eyeballing" the LCM-8 course relative to the surface floats.

In an attempt to estimate the magnitude of average systematic and random errors in **h** and **H** during the 100-foot-depth scans, a least-squares computer analysis of the Table 1 data was made. A FORTRAN program (Appendix B) was written to determine the set, $\{H_i, h_j\}$, which minimizes the mean-square error, ϵ, defined by

$$\epsilon = \frac{1}{N} \sum_{i=1}^{N} (\bar{y}_t - y_{ti})^2 \qquad (7)$$

where **N** = number of times the target is scanned

$$\bar{y}_t = \frac{1}{N} \sum_{i=1}^{N} y_{ti}$$

$y_{ti} = y_t$ for i^{th} computation

The results are given in Table 2. The average value of **h** is -17.25 feet, compared to -19.85 feet as computed from off-bottom fish heights (Table 1). The average value of **H** is 43.06 feet, as compared to

the assumed value of 42.00 feet. Random error in **h** is 7.5 feet; random error in **H** is 2.6 feet. Relative vertical fish oscillations of this magnitude could be expected, as can be seen in Figure 9, and because of the sensitivity of fish depth to tow speed. However, a random error in **H** of almost 3 feet is surprising, since there is no hydrodynamic reason to expect this. At any rate, the computed systematic and random errors in **h** and **H** explain the pronounced spread in y_t. An example calculation in Appendix A shows that an 0.5-foot error in each of the four parameters, R_1, R_2, **H**, and **h** yields an error of 3 feet in y_t for a 100-foot depth.

Table 3 gives the results of the one-time sweep of the Carpinteria rock outcroppings. A single sweep was made of a stretch of outcroppings approximately 4,000 feet long, running roughly parallel to the beach. No attempt was made to repeat this sweep because of the high probability of grounding one or both fish. The values of y_t (Table 3) were obtained in the same way as for Table 1. Figure 10 is a section of the stereo-sonar imagery obtained at the Carpinteria site.

There is a smaller spread in the y_t values in Table 3 than one would expect from using the small elevation angle, β_i. Since nominal water depth along the towing track was about 25 feet, 80% of the y_t values of Table 3 are possible. As shown in Figure 11, a least-squares linear fit to the y_t-versus-R_1 data yields a line having a slope of 3.9 degrees, which is not more than 2 degrees greater than the actual seafloor slope. The intercept (Figure 11) is 17.7 feet, which, again, is consistent with the actual depth of 25 feet, since the two fish were about 5 feet under the surface.

The imagery of the Carpinteria seafloor is highly photographic for the fish nearest the target (upper chart, Figure 10). However, the imagery from fish no. 2 is degraded, and it is impossible to fuse the two charts into a three-dimensional illusion.[e] The degradation is apparently caused by the interference of the near fish (no. 1) with the beam of the far fish (no. 2). Staggering the two fish was not possible by the technique used in the 100-foot scannings. Towing the two fish at different distances would have increased the likelihood of grounding.

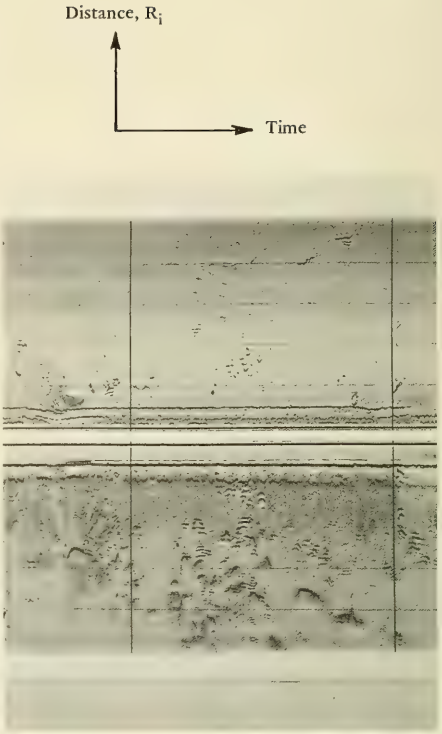

Distance between horizontal lines = 15 meters
Time between vertical lines = 2 minutes

Figure 10. Two-fish sonar-chart readout of rock outcroppings.

[e] Stereoscopic viewing would require that one of the charts be observed via a mirror, or made into a transparency and viewed from behind.

Table 2. Results of Least-Squares Analysis of 100-Foot-Depth Data

Target	H_i (ft)[a, b]	h_j (ft)[a, b]
SB1	45.50	-30.00
WR1	42.00	-12.00
SB2	44.00	-17.50
WR2	45.00	-13.00
SB3	37.00	-30.00
WR3	45.00	-12.50
SB4	42.50	-12.00
WR4	43.50	-12.00

[a] Average values: $\bar{H} = 43.06$ feet[c]
$\sigma_H = 2.57$ feet[d]
$\bar{h} = -17.25$ feet[c]
$\sigma_h = 7.53$ feet[d]

[b] $\{H_i, h_j\}$ is the set, consisting of the i^{th} value of H and the j^{th} value of h, which minimizes the mean-square error $\frac{1}{N}\sum_{i=1}^{N}(\bar{y}_t - y_{t_i})^2$, where $37.00 \leq H_i \leq 46.00$ and $12.00 \leq |h_j| \leq 30.00$.

[c] $\bar{x} = \frac{1}{N}\sum_{i=1}^{N} x_i$

[d] $\sigma_x^2 = \frac{1}{N}\sum_{i=1}^{N}(\bar{x} - x_i)^2$

N = number of times target elevation is computed.

Table 3. Results of Stereo-Sonar Scan of Rock Outcroppings

(Assumed value of horizontal stereo baseline, H, is 42.00 feet.)

Time	Outcropping Target	Fish No. 1 Echo Range, R_1 (ft)	Fish No. 2 Echo Range, R_2 (ft)	Fish Pair Depth Difference, h (ft)	Computed Target Elevation, y_t (ft)
1343	1	33.67	72.01	-2.59	24.21
1331	2	62.16	103.61	5.18	3.58
1331	3	102.57	141.94	5.18	27.31
1331	4	93.76	134.17	5.18	17.13
1331	5	53.36	88.58	4.66	28.34
1327	6	84.44	125.88	5.69	4.74
1342	7	65.79	109.30	0.00	0.00
1340	8	55.43	96.87	-1.55	15.74
1327	9	93.76	134.17	6.22	15.03
1325	10	44.03	85.48	6.73	0.26
1316	11	157.48	202.03	0.00	0.00

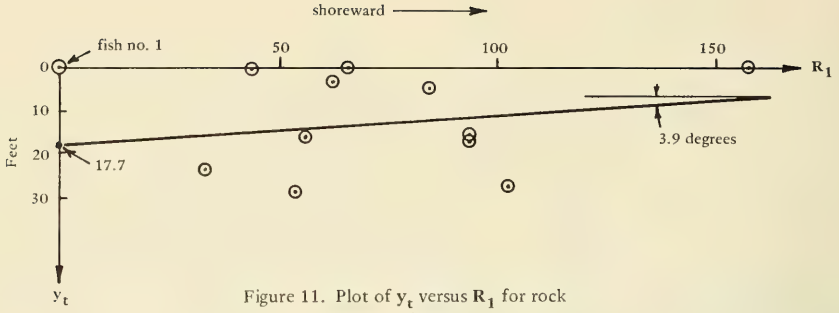

Figure 11. Plot of y_t versus R_1 for rock outcroppings.

A minor problem with the imagery of Figure 10 is that the return signal to each fish was produced by the outgoing pulse from the near fish.[f] This was, presumably, the result of mutual interference.

DISCUSSION

The results given in the preceding section clearly indicate that stereoscopic mapping of the seafloor from sonar data will require continuous and precise measurement of fish depths, separation, and lateral position in a fixed earth's reference frame. Because of the low rate of scanning the seafloor (the result of an energy propagation velocity of 5,000 ft/sec, compared to the velocity of light of 186,000 mi/sec), the only signal-processing approach to solving the slow-scan problem is some kind of automatic bridging process from one line scan to the next. This would only work for continuous targets extending throughout the swept area, for example, a long trench or cliff. Moreover, the circuitry needed for a bridging process of this sort would be more sophisticated than the circuitry and the acoustic transducers, combined, needed for measuring fish depth, fish separation, etc.

It is within the state-of-the-art to measure fish depths and fish separation with sufficient precision so that, with same-side stereo scanning, the relative target elevations are obtained with errors under 3 feet in 100 feet (see Appendix A). However, because of the likelihood of near-$\vec{B}$ points and the consequent large errors in y_t, it might be better to design a stereo-sonar system with a fish separation sufficiently large to allow opposite-side scanning. With continuous measurement of fish separation, the rigging and auxiliary structures for such a towing operation need not be too complicated. The idea of two manned catamarans connected by a crosstrack tension line might prove feasible. Large variations in separation distance during towing would be tolerable as long as the separation were precisely known for each line scan. The problem with opposite-side stereo scanning is, of course, that image correlation may be impossible for asymmetrical seafloor features, such as a cliff.

From the data obtained at the 100-foot-depth site the imagery problem can be avoided as long as fish heave, peak-to-peak, is less than 4 feet for echo ranges on the order of 100 feet. At greater depths, say 600 feet and more, as the result of greater tow-cable lengths vertical fish oscillations could be kept under 4 feet even in sea states higher than zero. Crosstalk or interference are no problem if tow distances are unequal; and, in low-flying sweeps in very shallow water (approximately 25 feet), controllable fins could be used to allow unequal trailing distances without danger of grounding.

Appendix C presents a description of a proposed analog signal-processing system which eliminates the need for interfacing a stereo operator's manipulations with a digital computer. The proposed system completely eliminates the need for fusing two sonar charts into a three-dimensional illusion; instead, the system produces in real time a readout equivalent to a stereo pair obtained photographically.

[f] Computation of target range, R_2, requires the equation:

$$R_2 = 2R_2' - R_1$$

where R_2' is the value read directly from the chart.

CONCLUSIONS

1. In a zero sea state, towing the two sonar fish at an average depth of 17 feet and average speed of 2 knots caused a random error of about 2.6 feet in the 43-foot horizontal baseline. Random error in the relative vertical separation of the two fish was around 7.5 feet. Even though the magnitude of these errors was probably a function of the particular sonar fish used in the investigation plus the physical parameters of the tow cable, the outrigger, and the towing vessel, it is concluded that, in same-side stereo, the depth of each fish and the lateral separation of the two fish must be continuously measured with a precision of about 0.5 foot in 40 feet.

2. In same-side stereo scanning, 100-kHz sonar imagery will be suitable for fusing into a three-dimensional illusion if the two fish are towed out of each other's beam and the heave for an individual fish is under 4 feet, peak-to-peak, at off-bottom heights around 70 feet.

RECOMMENDATIONS

An analog signal-processing system should be developed for producing an optical-stereo readout in real time from side-looking sonar returns. At-sea testing of this system should be conducted using a commercially available, side-scan system interfaced with conventional acoustic devices for continuously measuring fish depths and fish separation.

REFERENCES

1. J. R. Mittleman and R. J. Malloy. "Stereo side-scan sonar imagery," in Proceedings of Seventh Annual Conference of Marine Technology Society, Washington, D.C., Aug. 16-18 1971, pp. 395-422.

2. M. M. Thompson, Ed. Manual of photogrammetry, 3rd ed., vol. II. Falls Church, Va., American Society of Photogrammetry, 1966, pp. 1030-1035.

3. Naval Civil Engineering Laboratory. Technical Report 787: Rotating acoustic stereo scanner for positioning loads onto the seafloor: Preliminary observations on an experimental model, by R. D. Hitchcock. Port Hueneme, Calif., April 1973.

Appendix A

PROPAGATION OF MEASUREMENT ERRORS

The random error, σ_{y_t}, in relative elevation, y_t, is computed from the equation:

$$\sigma_{y_t}^2 = \sum_{i=1}^{4} \left(\frac{\partial y_t}{\partial \xi_i} \right)^2 \sigma_{\xi_i}^2 \qquad \text{(A-1)}$$

where $\xi_1 = R_1$

$\xi_2 = R_2$

$\xi_3 = H$

$\xi_4 = h$

From Equations 1 through 5 presented in the main text:

$$\frac{\partial y_t}{\partial R_1} = \frac{R_1}{B} \left[\sin\theta + \left(\frac{B + \xi}{\eta} \right) \cos\theta \right]$$

$$\frac{\partial y_t}{\partial R_2} = - \frac{R_2}{B} \left(\sin\theta + \frac{\xi}{\eta} \cos\theta \right)$$

$$\frac{\partial y_t}{\partial H} = \frac{1}{B^2} (H\xi + \eta h) \left[\sin\theta + \left(\frac{B + \xi}{\eta} \right) \cos\theta \right]$$

$$\frac{\partial y_t}{\partial h} = \frac{1}{B^2} (h\xi - \eta H) \left[\sin\theta + \left(\frac{B + \xi}{\eta} \right) \cos\theta \right]$$

Example calculation:

Let $R_1 = 83$ feet; $\sigma_{R_1} = 0.5$ foot

$R_2 = 121$ feet; $\sigma_{R_2} = 0.5$ foot

$H = 42$ feet; $\sigma_H = 0.5$ foot

$h = 20$ feet; $\sigma_h = 0.5$ foot

Therefore, $\partial y_t / \partial R_1 = 3.76$

$\partial y_t / \partial R_2 = -3.58$

$\partial y_t / \partial H = 3.58$

$\partial y_t / \partial h = -1.18$

$$\sigma_{y_t} = \sqrt{(0.5)^2 \left\{ (3.76)^2 + (3.58)^2 + (3.58)^2 + (1.18)^2 \right\}} = 3.2 \text{ feet}$$

Appendix B

FORTRAN PROGRAM FOR LEAST-SQUARES ANALYSIS OF TABLE 3 DATA

```
      DIMENSION R1SB1(2),R2SB1(2),R1SB2(4),R2SB2(4),R1SB3(5),R2SB3(5),
     1R1SB4(4),R2SB4(4),R1WR1(2),R2WR1(2),R1WR2(5),R2WR2(5),R1WR3(3),
     1R2WR3(3),R1WR4(3),R2WR4(3),H(19),ETA1(19),ETA2(19),Y(5),AYT(19,19,
     119),HN(8),EE(8),E(19,19,19),LHN(8)
      BF(A,B)=SQRT(A*A+B*B)
      XIF(A,B,C)=((A*A-B*B)/(2.*C))-(C/2.)
      ETAF(A,B)=SQRT(A*A-B*B)
      YTF(A,B,C,D)=-(A+B)*SIN(C)+D*COS(C)
      READ 1,R1SB1
      READ 1,R2SB1
      READ 2,R1SB2
      READ 2,R2SB2
      READ 3,R1SB3
      READ 3,R2SB3
      READ 2,R1SB4
      READ 2,R2SB4
      READ 1,R1WR1
      READ 1,R2WR1
      READ 3,R1WR2
      READ 3,R2WR2
      READ 4,R1WR3
      READ 4,R2WR3
      READ 4,R1WR4
      READ 4,R2WR4
      H0=37.0
      ETA10=23.0
      ETA20=2.0
      RSC=51.802
      DO 5 N=1,8
      IF (N-1) 6,6,7
    6 L1=2
      GO TO 8
    7 IF (N-2) 9,9,10
    9 L1=4
      GO TO 8
   10 IF(N-3) 11,11,12
   11 L1=5
      GO TO 8
   12 IF (N-4) 13,13,14
   13 L1=4
      GO TO 8
   14 IF(N-5) 15,15,16
   15 L1=2
      GO TO 8
```

```
16 IF(N-6) 17,17,18
17 L1=5
   GO TO 8
18 L1=3
 8 CONTINUE
   DO 19 I=1,15
   AI=I
   H(I)=0.5*(AI-1.0)+HJ
   DO 20 J=1,15
   AJ=J
   ETA1(J)=ETA10+0.5*(AJ-1.)
   DO 21 K=1,15
   AK=K
   ETA2(K)=ETA20+0.5*(AK-1.)
   HV=ETA2(K)-ETA1(J)
   B=BF(HV,H(I))
   A=ATAN(HV/H(I))
   AY=0.0
   DO 22 L=1,L1
   IF(N-1) 23,23,24
23 R1F=RSC*R1SB1(L)
   R2F=RSC*R2SB1(L)
   GO TO 25
24 IF(N-2) 26,26,27
26 R1F=RSC*R1SB2(L)
   R2F=RSC*R2SB2(L)
   GO TO 25
27 IF(N-3) 28,28,29
28 R1F=RSC*R1SB3(L)
   R2F=RSC*R2SB3(L)
   GO TO 25
29 IF(N-4) 30,30,31
30 R1F=RSC*R1SB4(L)
   R2F=RSC*R2SB4(L)
   GO TO 25
31 IF(N-5) 32,32,33
32 R1F=RSC*R1WK1(L)
   R2F=RSC*R2WK1(L)
   GO TO 25
33 IF(N-6) 34,34,35
34 R1F=RSC*R1WK2(L)
   R2F=RSC*R2WK2(L)
   GO TO 25
35 IF(N-7) 36,36,37
36 R1F=RSC*R1WK3(L)
   R2F=RSC*R2WK3(L)
   GO TO 25
37 R1F=RSC*R1WK4(L)
   R2F=RSC*R2WK4(L)
25 X1=XIF(R2F,R1F,B)
   IF(R1F-X1) 38,38,39
```

```
38 ETA=0.0
   XI=R1F
   GO TO 40
39 ETA=ETAF(R1F,XI)
40 YT=YTF(XI,B,A,ETA)
   Y(L)=YT+ETAZ(K)
   AY=AY+Y(L)
22 CONTINUE
   D=L1
   AYT(K,J,I)=AY/D
   ES=0.0
   DO 41 M=1,L1
   ES=ES+(AYT(K,J,I)-Y(M))**2
41 CONTINUE
   E(K,J,I)=SQRT(ES/D)
21 CONTINUE
20 CONTINUE
19 CONTINUE
   EMIN=999999.0
   DO 42 I=1,19
   DO 43 J=1,19
   DO 44 K=1,19
   EMIN=AMIN1(EMIN,E(K,J,I))
44 CONTINUE
43 CONTINUE
42 CONTINUE
   EE(N)=EMIN
   I=1
45 J=1
46 K=1
47 IF(EE(N)-E(K,J,I)) 48,49,48
48 IF(K-19) 50,51,51
51 IF(J-19) 52,53,53
53 IF(I-19) 54,55,55
50 K=K+1
   GO TO 47
52 J=J+1
   GO TO 46
54 I=I+1
   GO TO 45
55 CONTINUE
49 PRINT 56,ETA2(K),ETA1(J),H(I),AYT(K,J,I),EE(N)
   HN(N)=H(I)
   LHN(N)=ETA1(J)-ETA2(K)
 5 CONTINUE
   ALH=0.0
   AH=0.0
   AEE=0.0
   DO 57 N=1,8
```

```
      ALH=ALH+LHN(N)
      AH=AH+HN(N)
      AEE=AEE+EE(N)
   57 CONTINUE
      ALH=ALH/8.0
      AH=AH/8.0
      AEE=AEE/8.0
      SLH=0.0
      SH=0.0
      SEE=0.0
      DO 58 N=1,8
      SLH=SLH+(ALH-LHN(N))**2
      SH=SH+(AH-HN(N))**2
      SEE=SEE+(AEE-EE(N))**2
   58 CONTINUE
      SLH=SQRT(SLH/8.0)
      SH=SQRT(SH/8.0)
      SEE=SQRT(SEE/8.0)
      PRINT 59,ALH,SLH,AH,SH,AEE,SEE
    1 FORMAT (2F8.2)
    2 FORMAT (4F8.2)
    3 FORMAT (5F8.2)
    4 FORMAT (3F8.2)
   56 FORMAT (3F14.2,2F14.4)
   59 FORMAT (6F14.4)
      END
```

```
   2.27     2.28
   3.11     3.13
   1.82     2.07     2.67     1.97
   2.71     2.98     3.60     1.85
   2.83     1.70     2.14     2.77     1.95
   3.75     2.45     3.05     3.70     2.61
   2.26     2.42     2.34     1.93
   3.16     3.32     3.20     2.81
   2.33     2.35
   3.20     3.20
   1.97     1.89     2.18     2.76     1.20
   2.85     2.78     3.06     3.66     1.95
   2.67     3.00     2.20
   3.62     3.91     3.10
   2.39     2.51     2.04
   3.30     3.40     2.91
```

Appendix C

PROPOSED SYSTEM FOR ANALOG PROCESSING OF STEREO-SONAR SIGNALS[g]

The proposed system utilizes echo signals from a pair of towed side-scan sonar fish to generate, in real time, a roll of photographic film which can be directly viewed in a stereoscope to produce a true three-dimensional illusion of seafloor topography. The parallax in the stereo-photo image pairs will be optically true; that is, the image pairs will be the same as those obtained with a photographic stereo-camera. The system will, thus, make it possible to produce a seafloor contour map by the same technique used in stereo mapping of land contours. No digital computer will be required as in seafloor mapping from direct stereo-viewing of sonar charts.

The proposed system is an analog computer that uses a thin-film photoconductive liquid-crystal sandwich to produce a series of luminous points corresponding to off-track seafloor points. This series of points is imaged by means of a 3-to-2-dimensional fiber-optic static-scanning system onto the stereo-photo film, resulting in paris of stereoscopic traces of actual topography.

At a particular instant, the system images a pair of expanding, circular arcs onto the photoconductive liquid-crystal layered array. This array is capable of generating light only at the intersection point of the two arcs. The two circular arcs are initiated at the same instant that the two sonar pulses are initiated from the pair of towed fish. As the pulse from each fish moves out radially into the water, its wavefront has the shape of a circular arc; an optical image of each wavefront is reproduced within the system such that, at every instant, the radius of the optical image is proportional to the radius of the acoustic wavefront. Figure C-1 is a schematic of the system up to the liquid-crystal sandwich.

The system sequentially images certain intersection points of the two optically generated arcs onto a stereo-photo film. This imaging of the intersection points is the analog transformation of sonar signals to optical readout. This analog process computes the true target coordinates from the sonar parameters, $\mathbf{R_1}$, $\mathbf{R_2}$, and $\mathbf{B}$ (Figure 1), just as Equations 1 through 6 transform sonar to optical readout by means of a digital process.

The stereoscopic imaging process is performed by means of a static-scanning, fiber-optic assembly which maps each intersection point in the vertical plane of the sonar beam into a pair of stereo points on the crosstrack line in the plane of the photographic film. Figure C-2 is a schematic of the fiber-optics system.

The arc-intersection points imaged onto the photoconductive liquid-crystal sandwich represent the beginning of shadow regions along the crosstrack line. A given crosstrack line in a side-scan chart will contain blank or no-signal regions because of no energy being reflected from seafloor regions lying behind protuberances and outcroppings. These shadow regions produce negative derivatives in the echo signal. A circuit between the sonar transceiver and the optical-imaging system is responsive only to negative derivatives. Without this feature the system would image a multiplicity of arc-intersection points which would not be sensible on the photographic film.

The proposed system will work for any orientation of the fish-pair vector, $\vec{\mathbf{B}}$. If the vector, $\vec{\mathbf{B}}$, is continually changing in magnitude and direction during the tow, an additional device would be required to continually adjust the relative orientation of the arc-shaped slits. The successfulness of the proposed analog system, of course, depends on extremely high precision in the measurement of the tow-system parameters during each line scan.

[g] Invention Disclosure, Navy Case No. 57436 (patent application in preparation). The reader is referred to this Disclosure for a detailed narrative/pictorial description of the proposed system.

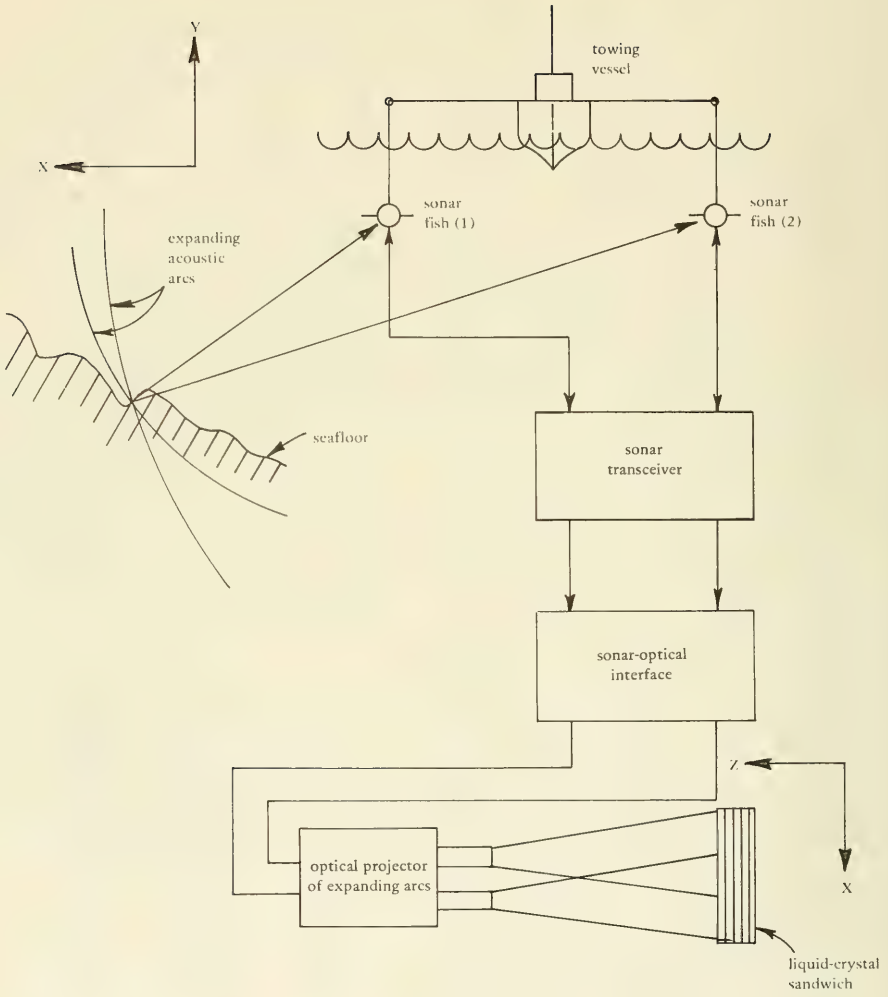

Figure C-1. Schematic of analog signal-processing up to Liquid Crystal Sandwich.

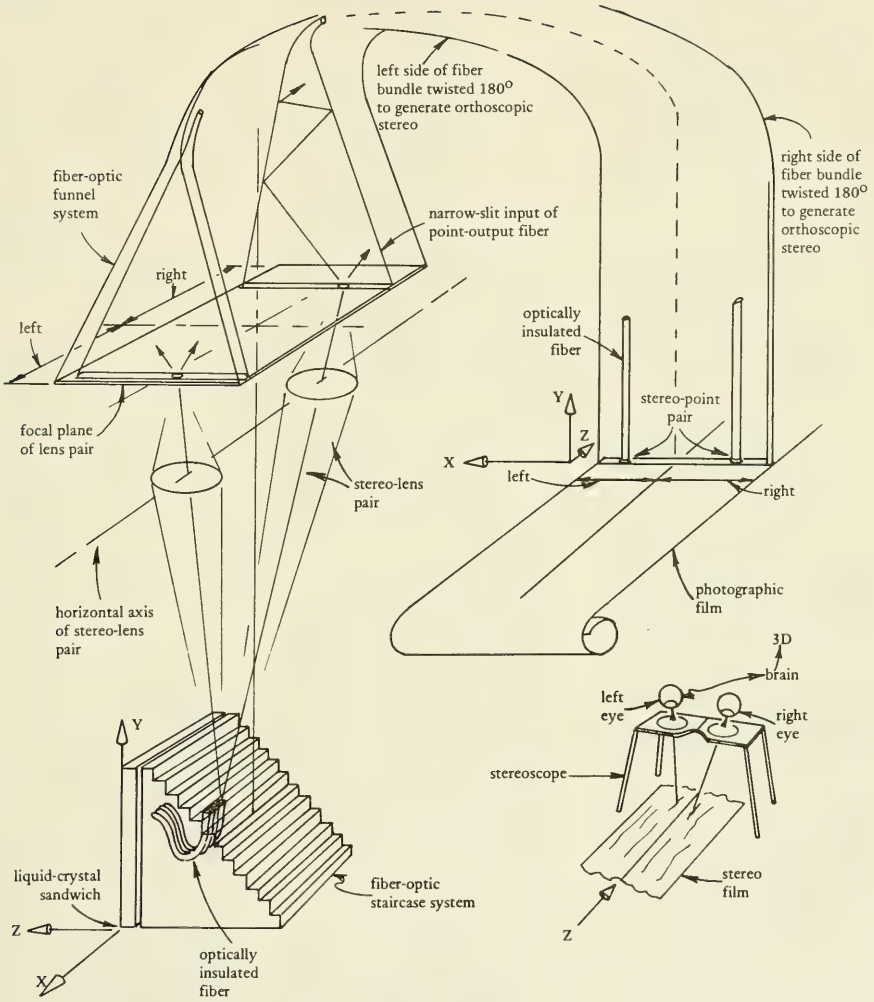

Figure C-2. Schematic of fiber-optics system.

DISTRIBUTION LIST

SNDL Code	No. of Activities	Total Copies	
—	1	12	Defense Documentation Center
—	1	1	Director of Navy Laboratories
FKAIC	1	3	Naval Facilities Engineering Command
FKNI	6	6	NAVFAC Engineering Field Divisions
FKN5	9	9	Public Works Centers
FA25	1	1	Public Works Center
—	9	9	RDT&E Liaison Officers at NAVFAC Engineering Field Divisions and Construction Battalion Centers
—	216	216	CEL Special Distribution List No. 11 for persons and activities interested in reports on Ocean Engineering

Bernard Willey (Code 385)*
Boston Naval Shipyard
Boston, MA 02129

LCDR David A. Cacchione, USN
Office of Naval Research, BROFF
495 Summer Street
Boston, MA 02210

Commanding Officer (Code 200)
Navy Public Works Center
Naval Base
Newport, RI 02840

President
Naval War College
Code 22
Newport, RI 02840

Mr. S. Milligan
SB 322
Naval Underwater Systems Center
Newport, RI 02844

Commander
21st Naval Construction Regiment
Davisville, RI 02854

Commanding Officer
CBC Technical Library
Naval Construction Battalion Center
Davisville, RI 02854 (2 copies)

Library
U. S. Army
Cold Regions Research & Eng. Lab.
P. O. Box 282
Hanover, NH 03755

Public Works Officer
Naval Security Group Activity
Winter Harbor, ME 04693

Public Works Department
Box 400
Naval Submarine Base, New London
Groton, CT 06340

LCDR T. A. Long, Jr., CEC, USN
Naval Submarine Base, New London
Groton, CT 06340

Commanding General
U. S. Army Electronics Command
Attn AMSEL-GG-TD
Fort Monmouth, NJ 07703

Engineering Director
Code 092
Naval Ammunition Depot, Earle
Colts Neck, NJ 07722

Plastics Technical Evaluation Center
SMUPA-VP3
Picatinny Arsenal
Dover, NJ 07801

Commanding Officer
Amphibious Construction Battalion TWO
FPO New York 09501

LT Ronald A. Milner, CEC, USN
U. S. Naval Station
Box 9
FPO New York 09540

Public Works Officer
U. S. Naval Facility
FPO New York 09552

Staff Civil Engineer
U. S. Naval Air Station
Box 35-D
FPO New York 09593

RDT&E Liaison Officer
Code 102
Northern Division
Naval Facilities Engineering Command
Philadelphia, PA 19112

Public Works Officer
Naval Facility
Lewes, DE 19958

Mr. R. B. Allnutt
Code 1706
Naval Ship Research & Dev. Center
Bethesda, MD 20034

Mr. M. A. Krenzke
Code 172 - Submarine Division
Naval Ship Research & Dev. Center
Bethesda, MD 20034

William F. Gerhold
National Bureau of Standards
Corrosion Section
Washington, DC 20234

A. Maillar
Maritime Administration
Office of Ship Construction
Washington, DC 20235

* All addressees receive one copy unless otherwise indicated.

Chief of Engineers
U. S. Army
DAEN-MCE-D
Washington, DC 20314

Benj. R. Petrie, Jr.
Op-987T8; Staff, Director RDT&E
Room 4B514, Pentagon
Washington, DC 20350

ENS James F. Morrow, CEC, USN
Office of Comptroller of the Navy
Navy Department
Washington, DC 20350

Commander
Naval Supply Systems Command
Headquarters
SUP 0423
Washington, DC 20360

Technical Library, Ships 2052
Naval Ship Systems Command
National Center No. 3
Washington, DC 20362

Commander
Naval Ship Systems Command
Code 00C
Washington, DC 20362

Chief
Bureau of Medicine & Surgery
Research Department
Navy Department
Washington, DC 20372

U. S. Naval Oceanographic Office
Library - Code 3600
Washington, DC 20373

John DePalma
U. S. Naval Oceanographic Office
Code 9233
Washington, DC 20373

Director
Code 2627
Naval Research Laboratory
Washington, DC 20375

Mr. J. P. Walsh
Naval Research Laboratory
Code 8400
Washington, DC 20375

Mr. J. J. Gennari
Naval Research Laboratory
Code 8410
Washington, DC 20375

Director of Navy Laboratories
Room 300, Crystal Plaza Bldg 5
Department of the Navy
Washington, DC 20376

Commanding Officer
Chesapeake Division - Code 03
Naval Facilities Engineering Command
Washington Navy Yard
Washington, DC 20390

CDR L. K. Donovan, CEC, USN
Chesapeake Division
Naval Facilities Engineering Command
Washington Navy Yard
Washington, DC 20390

Commandant
Naval District Washington
Public Works Department-Code 412
Washington, DC 20390

Naval Security Engineering Facility
Technical Library
3801 Nebraska Avenue, NW
Washington, DC 20390

Commandant (M-2/USP/83)
U. S. Coast Guard
400 SW 7th Street
Washington, DC 20590

Commander
Naval Ship Engineering Center
Code 6136
Prince Georges Center
Hyattsville, MD 20782

Commander
Naval Ship Engineering Center
Code 6162
Prince Georges Center
Hyattsville, MD 20782

Technical Library
Naval Ship Engineering Center
622 Center Bldg
Prince Georges Center
Hyattsville, MD 20782

Mr. John B. Alfers
Naval Ship Engineering Center
Code 6101E
Prince Georges Center
Hyattsville, MD 20782

Chief, Marine & Earth Sciences Library
National Oceanic & Atmospheric Admin.
Dept of Commerce
Rockville, MD 20852

M. E. Ringenbach
Engineering Development Lab (C61)
National Oceanic & Atmospheric Admin.
National Ocean Survey
Rockville, MD 20852

Mr. H. A. Perry
Naval Ordnance Laboratory, White Oak
Silver Spring, MD 20910

LCDR Robert D. Smart, CEC, USN
Naval System Engineering Dept
U. S. Naval Academy
Annapolis, MD 21402

Director
Division of Engineering & Weapons
U. S. Naval Academy
Annapolis, MD 21402

Dr Neil T. Monney
Naval Systems Engineering Dept
U. S. Naval Academy
Annapolis, MD 21402

Mr. D. H. Kallas
Annapolis Laboratory
Naval Ship Research & Dev. Center
Annapolis, MD 21402

Library, Code 5642
Annapolis Laboratory
Naval Ship Research & Dev. Center
Annapolis, MD 21402

Commanding Officer
U. S. Army Mobility Equip. R&D Center
Attn SMEFB-HPC (Mr. Cevasco)
Fort Belvoir, VA 22060

U.S. Army Coastal Eng. Research Center
Kingman Building
Fort Belvoir, VA 22060

U.S. Army Coastal Eng. Research Center
R.A. Jachowski
Kingman Building
Fort Belvoir, VA 22060

Facilities Officer
Code 108
Office of Naval Research
800 North Quincy Street
Arlington, VA 22217

LCDR G. E. Shank, CEC, USN
Office of Naval Research
Ocean Technology Program
800 North Quincy Street
Arlington, VA 22217

Dr Nicholas Perrone
Code 439
Office of Naval Research
800 North Quincy Street
Arlington, VA 22217

Dr Alexander Malahoff
Code 483
Office of Naval Research
800 North Quincy Street
Arlington, VA 22217

Oceanographer of the Navy
Attn: Code N712
200 Stovall Street
Alexandria, VA 22332

CAPT Pharo A. Phelps, CEC, USN
Naval Facilities Engineering Command
200 Stovall Street
Alexandria, VA 22332

Dr. Michael Yachnis
Code 04B
Naval Facilities Engineering Command
200 Stovall Street
Alexandria, VA 22332

CDR G.H. Gans, Jr., CEC, USN
Code 042
Naval Facilities Engineering Command
200 Stovall Street
Alexandria, VA 22332

Commander
Code 04B6
Naval Facilities Engineering Command
200 Stovall Street
Alexandria, VA 22332

CDR Walter J. Eager, CEC, USN
Code PC-2
Naval Facilities Engineering Command
200 Stovall Street
Alexandria, VA 22332

Mr. C.R. Odden
Code PC-2
Naval Facilities Engineering Command
200 Stovall Street
Alexandria, VA 22332

Commanding Officer
Navy Public Works Center
Norfolk, VA 23511

RDT&E Liaison Officer
Code 09P2
Atlantic Division
Naval Facilities Engineering Command
Norfolk, VA 23511 (2 copies)

Staff Civil Engineer
Commander Service Force
U. S. Atlantic Fleet
Norfolk, VA 23511

Director
Amphibious Warfare Board
Naval Amphibious Base, Little Creek
Norfolk, VA 23521

Commandant
U.S. Army Logistics Management Center
Attn DLSIE
Fort Lee, VA 23801

Public Works Officer
Naval Hospital
Camp Lejeune, NC 28542

RDT&E Liaison Officer
Southern Division - Code 90
Naval Facilities Engineering Command
P. O. Box 10068
Charleston, SC 29411

LCDR G. W. Callender, Jr., CEC, USN
NROTC Unit
Georgia Institute of Technology
Atlanta, GA 30332

Public Works Officer
Naval Coastal Systems Laboratory
Panama City, FL 32401

Mr. R. E. Elliott
Code 710
Naval Coastal Systems Laboratory
Panama City, FL 32401

Library Branch
Army Eng. Waterways Experiment Station
Vicksburg, MS 39180

Army Construction Eng. Research Lab.
ATTN Library
P.O. Box 4005
Champaign, IL 61820

Commanding Officer - Eng. Div.
MRD - Corps of Engineers
Department of the Army
P. O. Box 103, Downtown Station
Omaha, NE 68101

Public Works Officer
Naval Air Station, New Orleans
Belle Chasse, LA 70037

Public Works Officer
Naval Ammunition Depot
McAlester, OK 74501

LT H. S. Stevenson, CEC, USN
Texas A & M University
2304 Truman Street
Bryan, TX 77801

Dr. Arthur R. Laufer
Office of Naval Research, BROFF
1030 East Green Street
Pasadena, CA 91106

Public Works Officer
Marine Corps Base
Camp Pendleton, CA 92055

Mr. H. R. Talkington
Code 65
Naval Undersea Center
San Diego, CA 92132

Dr J. D. Stachiw
Code 6505
Naval Undersea Center
San Diego, CA 92132

Mr. R. E. Jones
Code 65402
Naval Undersea Center
San Diego, CA 92132

Technical Library
Code 1311
Naval Undersea Center
San Diego, CA 92132

Director
San Diego Branch
Western Division
Naval Facilities Engineering Command
San Diego, CA 92132

Public Works Officer
Code 75
Naval Undersea Center
San Diego CA 92132

Public Works Officer
Naval Air Station
North Island
San Diego, CA 92135

Staff Civil Engineer
Naval Station
San Diego, CA 92136

Commanding Officer
Navy Public Works Center
Naval Base
San Diego, CA 92136

Commanding Officer
Naval Missile Center
Code 5632.2, Technical Library
Point Mugu, CA 93042

Office of Patent Counsel
Code PC (Box 40)
Naval Missile Center
Point Mugu, CA 93042

Librarian, Code 9215
Construction Equipment Department
Naval Construction Battalion Center
Port Hueneme, CA 93043

Commanding Officer
Code 155
Naval Construction Battalion Center
Port Hueneme, CA 93043

Technical Library - Code C35
Naval School
Civil Engineer Corps Officers
Bldg 44
Port Hueneme, CA 93043

Commander
31st Naval Construction Regiment
Naval Construction Battalion Center
Port Hueneme, CA 93043 (2 copies)

Commander (Code 753)
Technical Library
Naval Weapons Center
China Lake, CA 93555

Superintendent
Attn Library (Code 2124)
Naval Postgraduate School
Monterey, CA 93940

Dr Edward B. Thornton
Department of Oceanography
Naval Postgraduate School
Monterey, CA 93940

Commanding Officer
Western Division - Code 09PA
Naval Facilities Engineering Command
P. O. Box 727
San Bruno, CA 94066

Commanding Officer
Western Division - Code 04
Naval Facilities Engineering Command
P. O. Box 727
San Bruno, CA 94066

Commanding Officer
Western Division - Code 04B
Naval Facilities Engineering Command
P. O. Box 727
San Bruno, CA 94066

Commanding Officer
Western Division - Code 05
Naval Facilities Engineering Command
P. O. Box 727
San Bruno, CA 94066

Commanding Officer
Western Division - Code 20
Naval Facilities Engineering Command
P. O. Box 727
San Bruno, CA 94066

Public Works Officer
Naval Station
Treasure Island
San Francisco, CA 94130

Asst. Resident OIC of Construction
Bldg 506
Hunters Point Naval Shipyard
San Francisco, CA 94135

Public Works Department (183)
Naval Air Station
Alameda, CA 94501

Supervisor of Salvage
West Coast Representative
4300 Eastshore Highway
Emeryville, CA 94608

Director, Engineering Division
Officer in Charge of Construction
Naval Facilities Engineering Command
Contracts, Southwest Pacific
APO San Francisco 96528

Headquarters
Kwajalein Missile Range
Box 26, Attn SSC-RKL-C
APO San Francisco 96555

Commanding Officer
Mobile Construction Battalion TEN
FPO San Francisco 96601

Operations Officer
Naval Construction Battalions
U. S. Pacific Fleet
FPO San Francisco 96610

Commander
Pacific Division
Naval Facilities Engineering Command
FPO San Francisco 96610

RDT&E Liaison Officer
Pacific Division - Code 403
Naval Facilities Engineering Command
FPO San Francisco 96610

Mr. T. M. Ishibashi
Navy Public Works Center
Engineering Department - Code 200
FPO San Francisco 96610

Public Works Officer
U. S. Naval Station
Box 15
FPO San Francisco 96614

Mr. D. K. Moore
Hawaii Laboratory
Naval Undersea Center
FPO San Francisco 96615

Officer in Charge of Construction
Naval Facilities Engineering Command
Contracts, Marianas
FPO San Francisco 96630

LT G.D. Cullison, CEC, USN
771 Murray Dr.
Honolulu, HI 96818

Engineering Library, Code 202.5
Puget Sound Naval Shipyard
Bremerton, WA 98314

Commanding Officer
U. S. Navy Public Works Center
Box 13
FPO Seattle 98762

Commanding Officer
U.S. Naval Air Facility
Box 15
FPO Seattle 98767

Colleges, etc

Prof. W. E. Heronemus
Civil Engineering Dept
University of Massachusetts
Amherst, MA 01002

MIT Libraries
Technical Reports - Room 14 E-210
Massachusetts Institute of Technology
Cambridge, MA 02139

Robert V. Whitman
Room 1-253
Massachusetts Institute of Technology
Cambridge, MA 02139

Mrs. A. P. Richards
Biological Sciences
William F. Clapp Labs - Battelle
Washington Street
Duxbury, MA 02332

Document Library L0-206
Woods Hole Oceanographic Institution
Woods Hole, MA 02543

Pell Marine Science Library
University of Rhode Island
Narragansett Bay Campus
Narragansett, RI 02882

Prof. R. W. Corell
Mechanical Engineering Dept.
Kingsbury Hall
University of New Hampshire
Durham, NH 03824

Kline Science Library
Kline Biology Tower, Room C-8
Yale University
New Haven, CT 06520

M. Schupack
Schupack Associates
300 Broad Street
Stamford, CT 06901

Mr. Willard J. Pierson, Jr.
University Institute of Oceanography
c/o The Bronx Community College
West 181st Street and University Ave.
Bronx, NY 10453

Reprint Custodian
Dept. of Nautical Science
U. S. Merchant Marine Academy
Kings Point, NY 11024

Dept of Civil Engineering
State University of New York
At Buffalo
Buffalo, NY 14214

Mr. R. F. Snyder
Ordnance Research Laboratory
Pennsylvania State University
State College, PA 16801

Mr. William H. Gotolski
Pennsylvania State University
212 Sackett Bldg
University Park, PA 16802

Professor Adrian F. Richards
Marine Geotechnical Laboratory
Lehigh University
Bethlehem, PA 18015

Associate Librarian
Mart Science & Engineering Library
Lehigh University
15 E. Packer Avenue
Bethlehem, PA 18015

Dr Hsuan Yeh
Towne School of Civil & Mechanical Eng.
University of Pennsylvania
Philadelphia, PA 19104

Professor E. Chesson
132 DuPont Hall
Newark, DE 19711

Professor Raymond R. Fox
Nuclear Defense Design Center
School of Engineering & Applied Science
The George Washington University
Washington, DC 20006

T. W. Mermel
4540 43rd Street, NW
Washington, DC 20016

Library of Congress
Science & Technology Division
Washington, DC 20540

Research Library
Chesapeake Bay Institute
The John Hopkins University
Macaulay Hall
Baltimore, MD 21218

W. F. Searle, Jr.
National Academy of Engineering
808 Timber Branch Parkway
Alexandria, VA 22302

Public Documents Department
Wm. R. Perkins Library
Duke University
Durham, NC 27706

Dr Aleksandar S. Vesic
Department of Civil Engineering
Duke University
Durham, NC 27706

Dr Bruce Muga
Dept of Civil Engineering
Duke University
Durham, NC 27706

Dr Wm F. Brumund
School of Civil Engineering
Georgia Institute of Technology
Atlanta, GA 30332

Professor J. P. Hartman
Dept of Civil Eng. & Environ. Sciences
Florida Technological University
Orlando, FL 32816

Dr Charles E. Lane
Institute of Marine Science
University of Miami
Coral Gables, FL 33146

Dr R. F. McAllister
Professor of Oceanography
Florida Atlantic University
Boca Raton, FL 33432

C. R. Stephan
Florida Atlantic University
Department of Oceanography
Boca Raton, FL 33432

Lorenz G. Straub Memorial Library
St Anthony Falls Hydraulic Laboratory
Mississippi River at 3rd Ave, SE
Minneapolis, MN 55414

Dr R. C. Jordan
Dept of Mechanical Engineering
University of Minnesota
Minneapolis, MN 55455

Library
Portland Cement Association
Research & Development Laboratories
5420 Old Orchard Road
Skokie, IL 60076

Dr N. M. Newmark
1114 Civil Engineering Bldg
University of Illinois
Urbana, IL 61801

Professor W. J. Hall
1108 Civil Engineering Bldg
University of Illinois
Urbana, IL 61801

Dr M. T. Davisson
2217 Civil Engineering Bldg
University of Illinois
Urbana, IL 61801

Metz Reference Room
Civil Engineering Dept
B106 Civil Engineering Bldg
University of Illinois
Urbana, IL 61801

Acquisition Dept - Serials Section
University of Nebraska Libraries
Lincoln, NE 68508

Robert D. Tent
Undersea Services Division
Fluor Ocean Services Inc
P. O. Drawer 310
Houma, LA 70360

Department of Oceanography
Texas A & M University
College Station, TX 77843

Civil Engineering Dept
Texas A & M University
College Station, TX 77843

R. C. Dehart
Southwest Research Institute
8500 Culebra Road
San Antonio, TX 78228

Director
Institute of Marine Science
The University of Texas
Port Aransas, TX 78373

Professor M. M. Ayoub
Dept of IE
Texas Technological University
Lubbock, TX 79409

Dr Bernard C. Abbott
Allan Hancock Foundation
University of Southern California
Los Angeles, CA 90007

Director
Catalina Marine Science Center
University of Southern California
Los Angeles, CA 90007

Aerospace Corporation
Acquisitions Group
P. O. Box 92957
Los Angeles, CA 90009

Dr Young C. Kim
Dept of Civil Engineering
Calif. State University, Los Angeles
Los Angeles, CA 90032

TRW Systems
Attn P. I. Dai R1/2178
1 Space Park
Redondo Beach, CA 90278

Mr. C. C. Mow
The Rand Corporation
1700 Main Street
Santa Monica, CA 90401

Dr. Armas Laupa
The Rand Corporation
1700 Main Street
Santa Monica, CA 90406

Robert Q. Palmer
P.O. Box 7707
Long Beach, CA 90807

Dr C. V. Chelapati
Calif. State University, Long Beach
Long Beach, CA 90840

Keck Reference Room (107-78)
136 W. M. Keck Laboratory
Calif. Institute of Technology
Pasadena, CA 91109

Oceanic Library & Info. Center
P. O. Box 2369
La Jolla, CA 92037

Dr John F. Peel Brahtz
P. O. Box 825
La Jolla, CA 92037

Mr. F. Simpson
Lockheed Ocean Laboratory
3380 No. Harbor Blvd
San Diego, CA 92101

Dr F. N. Spiess
Marine Physical Laboratory of the
Scripps Institution of Oceanography
University of California
San Diego, CA 92152

Dr Victor C. Anderson
Marine Physical Laboratory of the
Scripps Institution of Oceanography
University of California
San Diego, CA 92152

J. Padilla
866 Concord Ave
Ventura, CA 93003

Manager Ocean Systems, MVJG
Lockheed Missiles & Space Co
P. O. Box 504
Sunnyvale, CA 94088

Engineering Library
Stanford University Libraries
Stanford, CA 94305

Mr. Richard G. Luthy
615 Madison Street
Albany, CA 94706

Dept of Naval Architecture
College of Engineering
University of California
Berkeley, CA 94720

Engineering Library
University of California
Berkeley, CA 94720

Michael A. Taylor
Civil Engineering Dept
College of Engineering
University of California, Davis
Davis, CA 95616

Director
Calif. Dept of Navigation & Ocean Dev.
1416 9th Street
Sacramento, CA 95814

Assoc. Professor R. A. Grace
University of Hawaii
Honolulu, HI 96822

School of Oceanography
Oregon State University
Corvallis, OR 97331

Dr S. R. Murphy
University of Washington
Seattle, WA 98195

Information Officer
United Kingdom Scientific Mission
British Embassy
3100 Massachusetts Ave, NW
Washington, DC

Mrs. Ragna Adolfsson, Librarian
Cement-och Betonginstitutet
Fack 100 44 Stockholm 70
Sweden

Literature Exchange
Cement and Concrete Association
Wexham Springs
SLOUGH SL3 6PL
Bucks, England

Additions

LT J. M. Nelson, USN
Hawaii Laboratory (Code 1591)
Naval Undersea Center
FPO San Francisco 96615

Mr. Austin Kovacs
U.S. Army
Cold Regions Research & Eng. Lab.
P. O. Box 282
Hanover, NH 03755

Mr. John Quirk
Code 710
Naval Coastal Systems Lab.
Panama City, FL 32401

Public Works Dept.
Puget Sound Naval Shipyard
Bremerton, WA 98314

Mr. John R. Saroyan
1320 Carl Avenue
Vallejo, CA 94590

LCDR J. H. Osborn, CEC, USN
Code PME-124
Naval Electronic Systems Command
Washington, D.C. 20360

Director
Ocean Engineering Program Office
Naval Facilities Engineering Command
200 Stovall Street
Alexandria, VA 22332

Mr. Edmund Spencer
Ocean Engineering Program Office
Naval Facilities Engineering Command
200 Stovall Street
Alexandria, VA 22332

Technical Library
Naval Coastal Systems Laboratory
Panama City, FL 32401

Mr. R. G. Bea
Offshore Division—Construction
Shell Oil Company
P.O. Box 60124

LTJG W. M. Hall, CEC, USN
Dept of Ocean Engineering
University of Hawaii, Manolo Campus
Honolulu, HA 96622

LCDR James W. Eckert, CEC, USN
NROTC; NAU
Massachusetts Institute of Technology
Cambridge, MA 02139

Commanding Officer
Amphibious Const. Battalion 1
San Diego, CA 92155
Attn: Diving Officer

NOMENCLATURE

$\vec{B}$	Fish-pair vector
DS	Dynamic scattering (optical, in liquid crystal)
h	Vertical component of $\vec{B}$
H	Horizontal component of $\vec{B}$
N	Number of times target is scanned
OC	Outcropping
R_1	Echo range, fish no. 1
R_2	Echo range, fish no. 2
R_2'	Echo range, chart readout for OC data
SB	Sphere-block
t	Time
WR	Wire rope
x_t	Horizontal distance of target from fish no. 2
y_t	Vertical distance of target below fish no. 2
Z	Along-track distance
α	Sonar depression angle
β_i	Fish elevation angle
ϵ	Mean-square error
η	Value of y_t for $\theta = 0$
θ	Direction of $\vec{B}$
θ_s	Sonar beam angle, athwartship
ξ	Value of x_t for $\theta = 0$
ξ_i	Stereo-sonar parameter
σ	Random error

Civil Engineering Laboratory
STEREOSCOPIC MAPPING OF THE SEAFLOOR BY A TOWED TWO-FISH SIDE-SCAN SONAR SYSTEM, by R. D. Hitchcock
TR-813 27 p. illus June 1974 Unclassified

1. Seafloor mapping 2. Sonar mapping I. ZF61-512-001-025

Sea trials were conducted to test the concept of constructing a seafloor contour map by interfacing a manual stereo-sonar plotter with a digital computer. The at-sea work utilized a pair of 100-kHz, side-scan, sonar fish towed at a lateral separation of 42 feet. Real-time data on near-bottom scanning contained mutual interference effects which prevented the stereoscopic fusing of corresponding sonar images. System component errors were obtainable with repeated scannings of an artificial target array. Random errors in the horizontal component of the fish-pair vector, $\vec{B}$, were computed to be around 2.6 feet. Random errors in the vertical component of $\vec{B}$ were around 7.5 feet. These errors were associated with an average off-bottom distance of 70 feet and a fish-pair lateral separation of 43 feet. Because of the marked sensitivity of target-elevation error to the horizontal and vertical errors in $\vec{B}$, the stereo plotting of seafloor contours could not yield useful results. It is concluded that measurement of the components of $\vec{B}$ must yield errors less than 0.5 foot in 40 feet. It is further concluded that fish heave must be within 4 feet peak-to-peak and that mutual interference effects must be absent if stereo plotting of sonar-image pairs is to be performed successfully.

Civil Engineering Laboratory
STEREOSCOPIC MAPPING OF THE SEAFLOOR BY A TOWED TWO-FISH SIDE-SCAN SONAR SYSTEM, by R. D. Hitchcock
TR-813 27 p. illus June 1974 Unclassified

1. Seafloor mapping 2. Sonar mapping I. ZF61-512-001-025

Sea trials were conducted to test the concept of constructing a seafloor contour map by interfacing a manual stereo-sonar plotter with a digital computer. The at-sea work utilized a pair of 100-kHz, side-scan, sonar fish towed at a lateral separation of 42 feet. Real-time data on near-bottom scanning contained mutual interference effects which prevented the stereoscopic fusing of corresponding sonar images. System component errors were obtainable with repeated scannings of an artificial target array. Random errors in the horizontal component of the fish-pair vector, $\vec{B}$, were computed to be around 2.6 feet. Random errors in the vertical component of $\vec{B}$ were around 7.5 feet. These errors were associated with an average off-bottom distance of 70 feet and a fish-pair lateral separation of 43 feet. Because of the marked sensitivity of target-elevation error to the horizontal and vertical errors in $\vec{B}$, the stereo plotting of seafloor contours could not yield useful results. It is concluded that measurement of the components of $\vec{B}$ must yield errors less than 0.5 foot in 40 feet. It is further concluded that fish heave must be within 4 feet peak-to-peak and that mutual interference effects must be absent if stereo plotting of sonar-image pairs is to be performed successfully.

Civil Engineering Laboratory
STEREOSCOPIC MAPPING OF THE SEAFLOOR BY A TOWED TWO-FISH SIDE-SCAN SONAR SYSTEM, by R. D. Hitchcock
TR-813 27 p. illus June 1974 Unclassified

1. Seafloor mapping 2. Sonar mapping I. ZF61-512-001-025

Sea trials were conducted to test the concept of constructing a seafloor contour map by interfacing a manual stereo-sonar plotter with a digital computer. The at-sea work utilized a pair of 100-kHz, side-scan, sonar fish towed at a lateral separation of 42 feet. Real-time data on near-bottom scanning contained mutual interference effects which prevented the stereoscopic fusing of corresponding sonar images. System component errors were obtainable with repeated scannings of an artificial target array. Random errors in the horizontal component of the fish-pair vector, $\vec{B}$, were computed to be around 2.6 feet. Random errors in the vertical component of $\vec{B}$ were around 7.5 feet. These errors were associated with an average off-bottom distance of 70 feet and a fish-pair lateral separation of 43 feet. Because of the marked sensitivity of target-elevation error to the horizontal and vertical errors in $\vec{B}$, the stereo plotting of seafloor contours could not yield useful results. It is concluded that measurement of the components of $\vec{B}$ must yield errors less than 0.5 foot in 40 feet. It is further concluded that fish heave must be within 4 feet peak-to-peak and that mutual interference effects must be absent if stereo plotting of sonar-image pairs is to be performed successfully.

Civil Engineering Laboratory
STEREOSCOPIC MAPPING OF THE SEAFLOOR BY A TOWED TWO-FISH SIDE-SCAN SONAR SYSTEM, by R. D. Hitchcock
TR-813 27 p. illus June 1974 Unclassified

1. Seafloor mapping 2. Sonar mapping I. ZF61-512-001-025

Sea trials were conducted to test the concept of constructing a seafloor contour map by interfacing a manual stereo-sonar plotter with a digital computer. The at-sea work utilized a pair of 100-kHz, side-scan, sonar fish towed at a lateral separation of 42 feet. Real-time data on near-bottom scanning contained mutual interference effects which prevented the stereoscopic fusing of corresponding sonar images. System component errors were obtainable with repeated scannings of an artificial target array. Random errors in the horizontal component of the fish-pair vector, $\vec{B}$, were computed to be around 2.6 feet. Random errors in the vertical component of $\vec{B}$ were around 7.5 feet. These errors were associated with an average off-bottom distance of 70 feet and a fish-pair lateral separation of 43 feet. Because of the marked sensitivity of target-elevation error to the horizontal and vertical errors in $\vec{B}$, the stereo plotting of seafloor contours could not yield useful results. It is concluded that measurement of the components of $\vec{B}$ must yield errors less than 0.5 foot in 40 feet. It is further concluded that fish heave must be within 4 feet peak-to-peak and that mutual interference effects must be absent if stereo plotting of sonar-image pairs is to be performed successfully.

Civil Engineering Laboratory
STEREOSCOPIC MAPPING OF THE SEAFLOOR BY A TOWED TWO-FISH SIDE-SCAN SONAR SYSTEM, by R. D. Hitchcock
TR-813 27 p. illus June 1974 Unclassified

1. Seafloor mapping 2. Sonar mapping I. ZF61-512-001-025

Sea trials were conducted to test the concept of constructing a seafloor contour map by interfacing a manual stereo-sonar plotter with a digital computer. The at-sea work utilized a pair of 100-kHz, side-scan, sonar fish towed at a lateral separation of 42 feet. Real-time data on near-bottom scanning contained mutual interference effects which prevented the stereoscopic fusing of corresponding sonar images. System component errors were obtainable with repeated scannings of an artificial target array. Random errors in the horizontal component of the fish-pair vector, $\vec{\mathbf{B}}$, were computed to be around 2.6 feet. Random errors in the vertical component of $\vec{\mathbf{B}}$ were around 7.5 feet. These errors were associated with an average off-bottom distance of 70 feet and a fish-pair lateral separation of 43 feet. Because of the marked sensitivity of target-elevation error to the horizontal and vertical errors in $\vec{\mathbf{B}}$, the stereo plotting of seafloor contours could not yield useful results. It is concluded that measurement of the components of $\vec{\mathbf{B}}$ must yield errors less than 0.5 foot in 40 feet. It is further concluded that fish heave must be within 4 feet peak-to-peak and that mutual interference effects must be absent if stereo plotting of sonar-image pairs is to be performed successfully.

Civil Engineering Laboratory
STEREOSCOPIC MAPPING OF THE SEAFLOOR BY A TOWED TWO-FISH SIDE-SCAN SONAR SYSTEM, by R. D. Hitchcock
TR-813 27 p. illus June 1974 Unclassified

1. Seafloor mapping 2. Sonar mapping I. ZF61-512-001-025

Sea trials were conducted to test the concept of constructing a seafloor contour map by interfacing a manual stereo-sonar plotter with a digital computer. The at-sea work utilized a pair of 100-kHz, side-scan, sonar fish towed at a lateral separation of 42 feet. Real-time data on near-bottom scanning contained mutual interference effects which prevented the stereoscopic fusing of corresponding sonar images. System component errors were obtainable with repeated scannings of an artificial target array. Random errors in the horizontal component of the fish-pair vector, $\vec{\mathbf{B}}$, were computed to be around 2.6 feet. Random errors in the vertical component of $\vec{\mathbf{B}}$ were around 7.5 feet. These errors were associated with an average off-bottom distance of 70 feet and a fish-pair lateral separation of 43 feet. Because of the marked sensitivity of target-elevation error to the horizontal and vertical errors in $\vec{\mathbf{B}}$, the stereo plotting of seafloor contours could not yield useful results. It is concluded that measurement of the components of $\vec{\mathbf{B}}$ must yield errors less than 0.5 foot in 40 feet. It is further concluded that fish heave must be within 4 feet peak-to-peak and that mutual interference effects must be absent if stereo plotting of sonar-image pairs is to be performed successfully.

Civil Engineering Laboratory
STEREOSCOPIC MAPPING OF THE SEAFLOOR BY A TOWED TWO-FISH SIDE-SCAN SONAR SYSTEM, by R. D. Hitchcock
TR-813 27 p. illus June 1974 Unclassified

1. Seafloor mapping 2. Sonar mapping I. ZF61-512-001-025

Sea trials were conducted to test the concept of constructing a seafloor contour map by interfacing a manual stereo-sonar plotter with a digital computer. The at-sea work utilized a pair of 100-kHz, side-scan, sonar fish towed at a lateral separation of 42 feet. Real-time data on near-bottom scanning contained mutual interference effects which prevented the stereoscopic fusing of corresponding sonar images. System component errors were obtainable with repeated scannings of an artificial target array. Random errors in the horizontal component of the fish-pair vector, $\vec{\mathbf{B}}$, were computed to be around 2.6 feet. Random errors in the vertical component of $\vec{\mathbf{B}}$ were around 7.5 feet. These errors were associated with an average off-bottom distance of 70 feet and a fish-pair lateral separation of 43 feet. Because of the marked sensitivity of target-elevation error to the horizontal and vertical errors in $\vec{\mathbf{B}}$, the stereo plotting of seafloor contours could not yield useful results. It is concluded that measurement of the components of $\vec{\mathbf{B}}$ must yield errors less than 0.5 foot in 40 feet. It is further concluded that fish heave must be within 4 feet peak-to-peak and that mutual interference effects must be absent if stereo plotting of sonar-image pairs is to be performed successfully.

Civil Engineering Laboratory
STEREOSCOPIC MAPPING OF THE SEAFLOOR BY A TOWED TWO-FISH SIDE-SCAN SONAR SYSTEM, by R. D. Hitchcock
TR-813 27 p. illus June 1974 Unclassified

1. Seafloor mapping 2. Sonar mapping I. ZF61-512-001-025

Sea trials were conducted to test the concept of constructing a seafloor contour map by interfacing a manual stereo-sonar plotter with a digital computer. The at-sea work utilized a pair of 100-kHz, side-scan, sonar fish towed at a lateral separation of 42 feet. Real-time data on near-bottom scanning contained mutual interference effects which prevented the stereoscopic fusing of corresponding sonar images. System component errors were obtainable with repeated scannings of an artificial target array. Random errors in the horizontal component of the fish-pair vector, $\vec{\mathbf{B}}$, were computed to be around 2.6 feet. Random errors in the vertical component of $\vec{\mathbf{B}}$ were around 7.5 feet. These errors were associated with an average off-bottom distance of 70 feet and a fish-pair lateral separation of 43 feet. Because of the marked sensitivity of target-elevation error to the horizontal and vertical errors in $\vec{\mathbf{B}}$, the stereo plotting of seafloor contours could not yield useful results. It is concluded that measurement of the components of $\vec{\mathbf{B}}$ must yield errors less than 0.5 foot in 40 feet. It is further concluded that fish heave must be within 4 feet peak-to-peak and that mutual interference effects must be absent if stereo plotting of sonar-image pairs is to be performed successfully.